Journal of Power Sources 196 (2011) 868–871

Contents lists available at ScienceDirect

Journal of Power Sources

journal homepage: www.elsevier.com/locate/jpowsour

Short communication

A-site deficient $Ba_{1-x}Co_{0.7}Fe_{0.2}Ni_{0.1}O_{3-\delta}$ cathode for intermediate temperature SOFC

Ze Liu, Ling-zhi Cheng, Min-Fang Han*

Union Research Center of Fuel Cell, School of Chemical & Environment Engineering, China University of Mining & Technology (CUMTB), Beijing 100083, PR China

ARTICLE INFO

Article history:
Received 20 April 2010
Received in revised form 25 May 2010
Accepted 26 May 2010
Available online 31 May 2010

Keywords:
Solid oxide fuel cell
$Ba_{1-x}Co_{0.7}Fe_{0.2}Ni_{0.1}O_{3-\delta}$
Cathode
A-site deficient

ABSTRACT

A-site cation-deficient $Ba_{1-x}Co_{0.7}Fe_{0.2}Nb_{0.1}O_{3-\delta}$ (B_{1-x}CFN, $x = 0.00$–0.15) oxides are synthesized and evaluated as cathode materials for intermediate temperature solid oxide fuel cells (IT-SOFCs). The reactivity between B_{1-x}CFN and gadolinia doped ceria (GDC) is observed at different temperature, and no second phase is detected under 1050 °C. The increasing in A-site cation deficiency results in a steady decrease in cathode polarization resistance. Among the various B_{1-x}CFN oxides test, GDC based anode supported cells with $B_{0.9}$CFN cathode possess the smallest interfacial polarization resistance (R_p). The R_p is as low as 0.283 and 0.046 Ω cm^2 at 500 and 600 °C, respectively. The anode supported cell with $B_{0.9}$CFN provides maximum power densities of 1062 and 1139 mW cm^{-2} at 600 and 650 °C, respectively. The results suggest that $B_{0.9}$CFN is a great potential cathode material for IT-SOFCs.

1. Introduction

The performance of a traditional solid oxide fuel cell (SOFC) is often limited by the oxygen reduction processes at the cathode [1,2]. This is especially true for SOFC based on thin-electrolyte and operated in H_2 fuel, where the resistances of the electrolyte and anode are relatively small [3,4]. Perovskite materials, such as ABO_3-type oxides with A = Ln (lanthanides), Ca, Sr, Ba; B = Cr, Mn, Fe, Co, Ni, Ga, In, and with mixed occupation of the A- and B-lattices [5], are often available for cathode. $Ba_{0.5}Sr_{0.5}Co_{0.8}Fe_{0.2}O_{3-\delta}$ (BSCF) exhibits good performance at low temperature [6], but it is limited by the poor stability in carbon dioxide [7,8]. A full or partial substituting of Sr by Ba in A-site will result in the larger free volume of perovskite due to the larger ionic radius of barium than strontium, and larger specific free volume will offer a large transportation path for oxygen ions, which will enhance the diffusion of oxygen in bulk and improve the oxygen ion conductivity [9]. To enhance the structure stability of $BaCoO_{3-\delta}$-based perovskites, one strategy is to dope their B-site via proper cations. Nagai et al. demonstrated that Nb is the most effective dopant in B-site for improving the phase stability of the Co-based perovskite oxides [10]. $BaCo_{0.7}Fe_{0.2}Nb_{0.1}O_{3-\delta}$ (BCFN) as a cathode exhibits the high electrocatalytic activity for oxygen reduction which shows about 1 W cm^{-2} at 800 °C [11]. On the other hand, some researchers have found that A-site cation deficiencies introduced into the lattice structure of perovskite oxides significantly affects the physical and chemical properties of materials. A-site cation-deficient cathode $(La_{0.6}Sr_{0.4})_{1-x}Co_{0.2}Fe_{0.8}O_{3-\delta}$, shows a lower electronic conductivity than the corresponding cation-stoichiometric material ($La_{0.6}Sr_{0.4}Co_{0.2}Fe_{0.8}O_{3-\delta}$) [12]. Doshi et al. observed that the initial cathode resistance of A-site cation-deficient LSCF cathodes was as low as 0.1 Ω cm^2 at 500 °C [13]. Mineshige et al. suggested that the reduced electronic conductivity could be attributed to the creation of additional oxygen vacancies [14]. Very recently, it was indicated that additional oxygen vacancies were indeed beneficial to the oxygen reduction reaction [15]. Shao and Haile demonstrated that creating additional oxygen vacancies from the A-site deficiencies of $Ba_{0.5}Sr_{0.5}Co_{0.8}Fe_{0.2}O_{3-\delta}$ facilitated oxygen ion diffusion within the oxide bulk, and that this effect was responsible for the improved oxygen permeability of the related membranes [16].

In this study, we systematically evaluated the effect of A-site cation deficiency on the performance of $Ba_{1-x}Co_{0.7}Fe_{0.2}Ni_{0.1}O_{3-\delta}$ (B_{1-x}CFN) ($x = 0$–0.15) perovskite cathodes in IT-SOFC fabricated with a gadolinia doped ceria (GDC) electrolyte. The phase reaction between the cathode and the electrolyte of these materials and electrochemical properties were investigated. Our results show A-site deficient B_{1-x}CFN is a great potential cathode material for IT-SOFC.

2. Experimental

A-site deficient $Ba_{1-x}Co_{0.7}Fe_{0.2}Nb_{0.1}O_{3-\delta}$ composite oxides ($x = 0$–0.15) were synthesized by solid-state reaction method. The stoichiometric amounts of $BaCO_3$, Co_3O_4, Fe_2O_3, and Nb_2O_5 (99.9%,

* Corresponding author at: Union Research Center of Fuel Cell, School of Chemical & Environment Engineering, China University of Mining & Technology (CUMTB), Box 8, Xueyuan Rd Ding 11, Haidian District, Beijing, PR China. Tel.: +86 10 62341427.
E-mail address: hanminfang@sina.com (M.-F. Han).

0378-7753/$ – see front matter.
doi:10.1016/j.jpowsour.2010.05.051

Lanyi Coop., Beijing) were mixed and milled in ethanol for 24 h. The dried precursors were calcined at 1000 °C for 12 h in air. Then the powders were ball-milled again for 12 h to achieve average particle distribution. The cathode slurries were prepared by mixing and milling with a mount of ethyl cellulose and terpineol for 12 h.

NiO/GDC anode substrate and GDC electrolyte were tape-cast separately, then dried in air at room temperature for 12 h. The electrolyte and anode substrate tapes were isostatic pressed at 16 MPa by 30 T thermal isostatic press (China), and sintered at 1350 °C for 5 h. The B_{1-x}CFN cathode was screen printed on the GDC electrolyte, then sintered at 1050 °C for 3 h. The electrode active area was 0.2 cm^2. The single cell was sealed on an alumina tube. Electrochemical characterizations were performed at temperatures from 500 to 700 °C under ambient pressure. Fuel cell performances were measured with IM6 & Zennium analyzer. Humidified (3% H_2O) hydrogen with 80 ml min^{-1} was used as fuel and stationary air as oxidant. The impedances were measured typically in the frequency range from 0.01 Hz to 1 MHz. The microstructures of BCFN cathodes were observed by thermally-assisted field emission scanning electron microscope (FEI XL30 S-FEG). Phase identification was carried out on PANalytical X'Pert PRO X-ray diffractometer using Cu Kα radiation.

3. Results and discussion

Fig. 1 shows the X-ray diffraction pattern of B_{1-x}CFN (x = 0–0.15) after calcinations at 1000 °C in air for 24 h. The oxides with x = 0–0.15 possess a perovskite phase structure with cubic symmetry. As the A-site cation deficiency increases up to values of x = 0.15, the main diffraction peaks of the B_{1-x}CFN perovskite gradually shift to higher values of 2θ, which indicates shrinkage of the perovskite lattice. Whereas the impurity Co_3O_4 was found in $B_{0.85}$CFN pattern, therefore $B_{0.85}$CFN will not be evaluated in this study. And it is suggested that the A-site cation deficiency fraction (x) was limited to approximately 0.1 for B_{1-x}CFN. Undesirable reaction in the composite cathode may degrade the electrode electrical characteristic, sinterability and strength [17]. X-ray diffractograms for B_{1-x}CFN–GDC mixed powders taken before and after 10 h reaction at 1000–1100 °C. The XRD patterns of reaction between GDC and $B_{1.0}$CFN are typically presented in Fig. 2a. Impurity $BaCeO_3$ was detected after fired $B_{1.0}$CFN–GDC power at 1100 °C for 10 h and there is no reaction between GDC and $B_{1.0}$CFN blew 1050 °C. Because A-site deficient BCFN is mainly investigated in this paper,

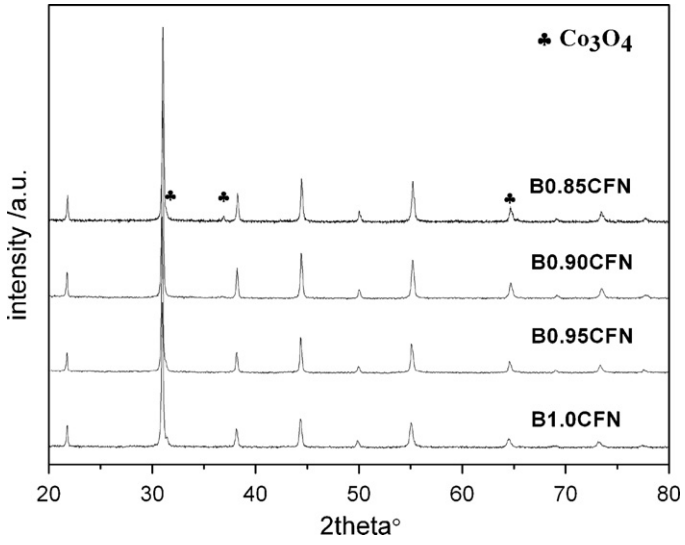

Fig. 1. XRD patterns of B_{1-x}CFN powders (x = 0–0.15).

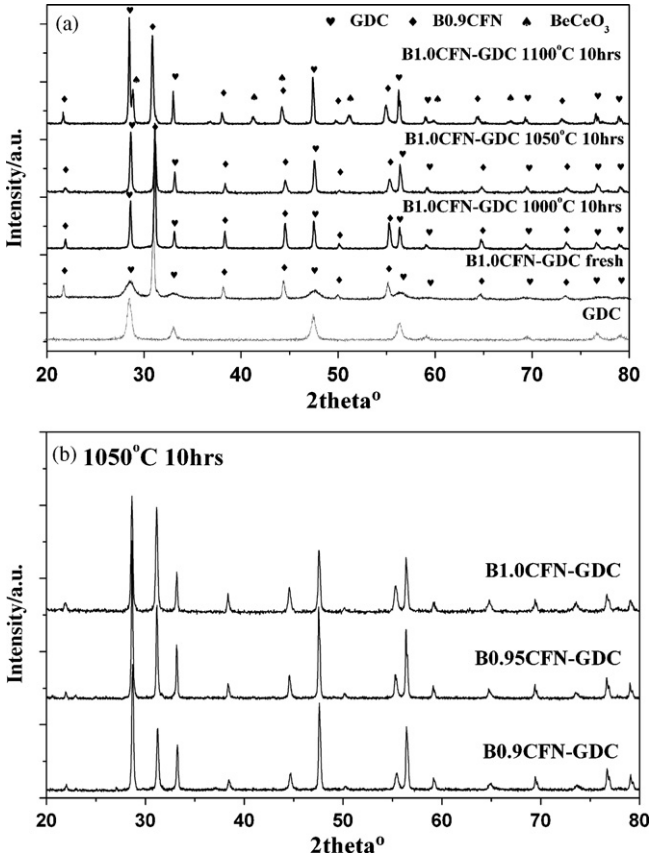

Fig. 2. XRD patterns of reaction between B_{1-x}CFN and GDC powders at different temperature: (a) $B_{1.0}$CFN-GDC and (b) B_{1-x}CFN-GDC at 1050 °C for 10 h.

the same results were achieved in GDC-$B_{0.95}$CFN and GDC-$B_{0.9}$CFN at 1050 °C, as shown in Fig. 2b. Thus, it is reasonable to conclude that B_{1-x}CFN is a suitable and chemically stable cathode material for GDC electrolyte.

Fig. 3 shows cross-section and surface morphologies of BCFN cathode in anode supported GDC cell. The dense GDC electrolyte is about 20 μm and the average thickness of the cathode layer is approximately 25 μm. It can be seen that the cathode is homogeneous with a porosity about 30%, which can ensure smooth transport of the gases. The interface image indicates strong bonding between porous cathode and dense GDC electrolyte. No delamination occurs at the electrolyte–cathode interface after long term cell testing.

The performance of B_{1-x}CFN (x = 0.00, 0.05, and 0.10, fired at 1050 °C) as the cathode via AC impedance spectroscopy in anode supported cells were investigated under air condition. The Nyquist plots of the cells were obtained at 600 °C at open-circuit conditions, as shown in Fig. 4a. Each spectrum was collected about 1 h after the cell reached a steady state. The differences of all bulk resistances were within the range of 5%. In order to show the polarization resistance clearly, all bulk resistances were normalized to zero. The polarization resistances of the electrode–electrolyte interfaces include the resistances of anode (R_A) and cathode (R_C). The difference of cathode interfacial resistance of B_{1-x}CFN is approximate to the difference of total interfacial resistances ($R_A + R_C$) in anode supported cells, because of the same anode interfacial resistances. The increase of Ba deficient concentration causes a significantly decrease in the total interfacial polarization resistance. When the Ba deficient concentration increases up to 0.10, the total interfacial polarization decreased about 51.9%, from 0.096 to 0.046 Ω cm^2, which is mainly attributed to the decrease of cathode interfacial

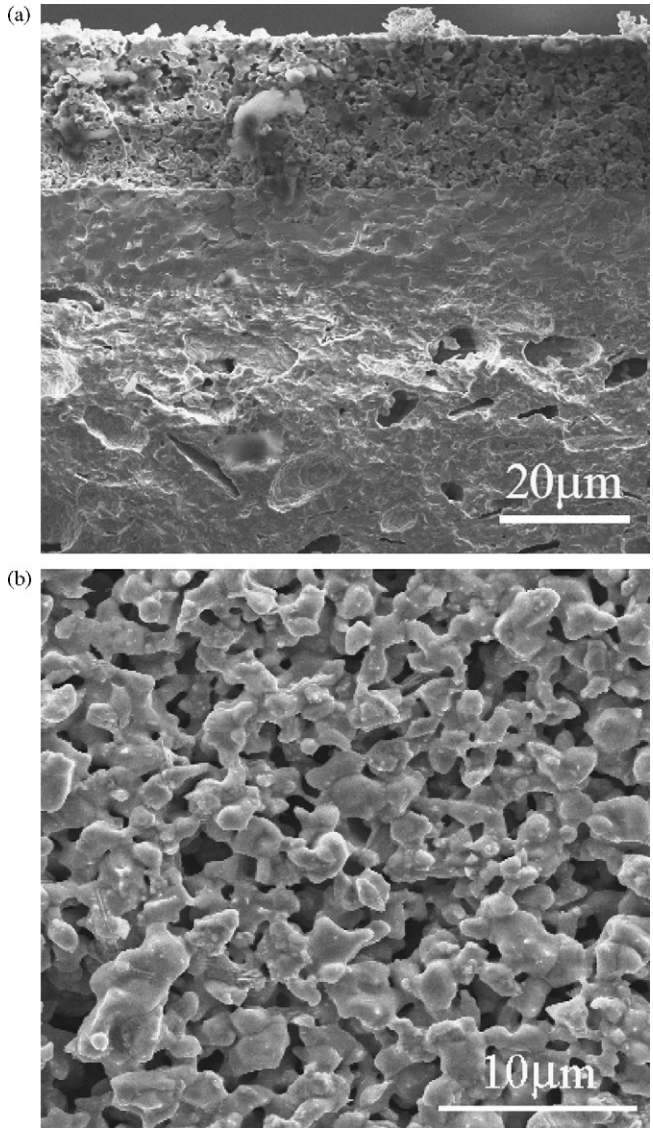

Fig. 3. SEM of Ni-GDC/GDC/BCFN cell. (a) Cross-section of BCFN, 2K×; (b) surfaces of BCFN, 5K×.

resistance. The defect of Ba content induces the preferential formation of oxygen vacancies and promotes oxygen surface-exchange processes [16]. The temperature dependence of the cathode polarization resistances for B_{1-x}CFN is shown in Fig. 4b. Increasing the A-site cation deficiency creates more oxygen vacancies, which is beneficial to the oxygen reduction reaction [15], and results in the area specific resistances of the cathode decreasing. Although the active energy of $B_{0.9}$CFN is higher than $B_{0.95}$CFN and $B_{1.0}$CFN, the interfacial resistances of $B_{0.9}$CFN are lower than $B_{0.95}$CFN and $B_{1.0}$CFN in the operation temperature of 500–650 °C, which means $B_{0.9}$CFN is a better cathode for IT-SOFC.

The $B_{0.9}$CFN material displays the good performance for application in SOFCs, because it indicates high electrocatalytic oxygen reduction activity. The performances of anode supported cells with B_{1-x}CFN cathode were then measured in terms of their respective power and current densities using humidified H_2 (3% H_2O) as the fuel and ambient air as the oxidant at temperatures between 500 and 650 °C. The comparison of cell performances of B_{1-x}CFN at 600 °C was shown in Fig. 5. When the Ba deficient concentrations of B_{1-x}CFN increased from 0 to 0.10, the peak power densities enhanced about 31.7% at 600 °C, from 806 to 1062 mW cm^{-2}. Fig. 6

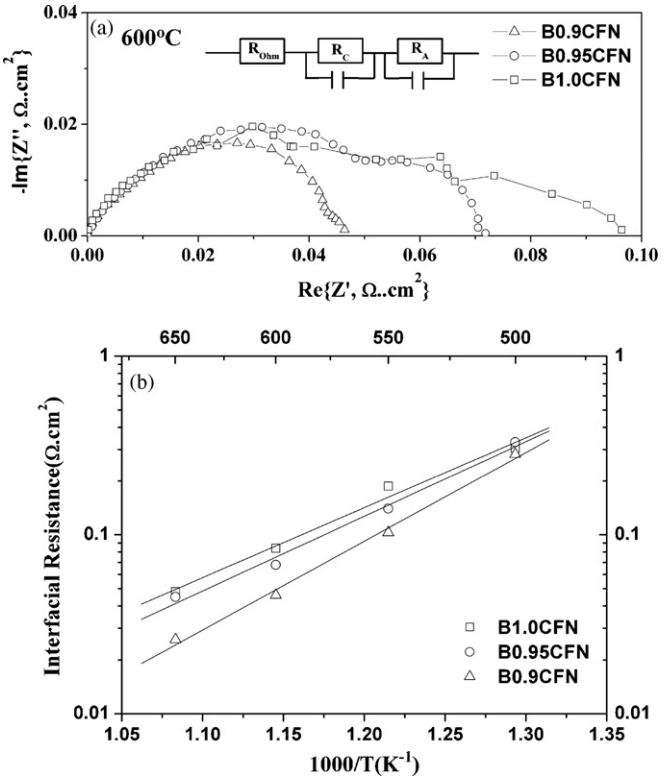

Fig. 4. Temperature dependence of R_p for Ba_{1-x}CFN (x = 0–0.10) cathode. (a) Nyquist-type impedance curves at 600 °C; (b) temperature dependence of R_p.

shows the performance and impedance of $B_{0.9}$CFN based anode supported cell. It is achieved that peak power densities of 1062 and 1139 mW cm^{-2} at 600 and 650 °C, respectively. The total electrode polarization resistance was measured under OCV conditions. The electrode interfacial resistances employed with the $B_{0.9}$CFN cathode are only 0.046 and 0.026 Ω cm^2 at 600 and 650 °C in the cell respectively. At intermediate temperature, $B_{0.9}$CFN exhibited higher charge-transfer process of oxygen reduction and mass-transfer. The optimized A-site cation-deficient material, $B_{0.9}$CFN, is a promising new cathode material for application in IT-SOFCs.

Actually, BCFN system cathode materials cannot only be used in oxygen ion conductor IT-SOFC, but also proton conductor SOFC. Liu et al. [18,19] developed composite cathodes, e.g. $Sm_{0.5}Sr_{0.5}CoO_{3-\delta}$ (SSC)/$Ba(Zr_{0.1}Ce_{0.7}Y_{0.2})O_{3-\delta}$(BZCY) and $La_{0.6}Sr_{0.4}Co_{0.2}Fe_{0.8}O_{3-\delta}$ (LSCF)/BZCY, and demonstrated high performance in proton conductor anode supported cell at 500–750 °C,

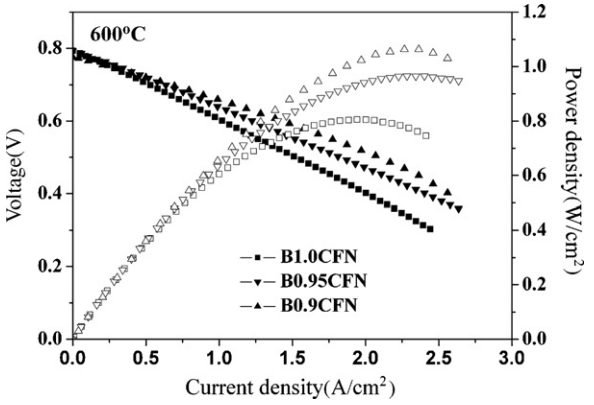

Fig. 5. The comparison of cell performance of Ba_{1-x}CFN (x = 0–0.10) cathode at 600 °C.

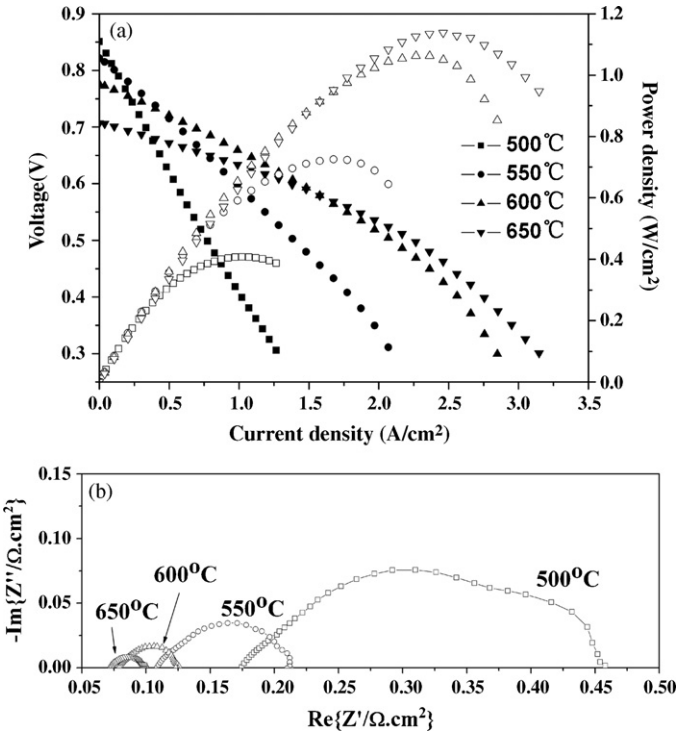

Fig. 6. The performance of $B_{0.9}$CFN based anode supported cell. (a) *I–V* and *I–P* curves of Cell performance; (b) Nyquist-type impedance curves.

while there are new phase formed between SSC and BZCY, such as $BaCoO_3$, $Sm_2Zr_2O_7$, at 1000 °C. BCFN and BZCY are all Ba-based perovskite materials, and there is no reaction between BCFN and BZCY at 1000 °C. BCFN can be individually or compositely employed as cathode in $BaCeO_3$ based proton conductor cell. This work will be demonstrated in the future.

4. Conclusions

$Ba_{1-x}Co_{0.7}Fe_{0.2}Nb_{0.1}O_{3-\delta}$ (B_{1-x}CFN, x = 0.00–0.15) oxides have been proved as cathode materials for its great potential application in IT-SOFCs. B_{1-x}CFN forms pure cubic perovskite structure at y = 0–0.10. No second phase forms between B_{1-x}CFN and GDC at 1050 °C. The $B_{0.9}$CFN cathode exhibits the lowest polarization resistance at the measured temperatures. The polarization resistance is only 0.046 and 0.026 Ω cm^2 at 600 and 650 °C in GDC based anode supported cell with $B_{0.9}$CFN cathode. The maximum power density of the cell using $B_{0.9}$CFN reaches 1062 and 1139 mW cm^{-2} at 600 and 650 °C, respectively.

Acknowledgements

Financial support from the NSFC key project (50730004), MOST projects (No. 2006AA11A189 and 2009DFA6136) and MOE project (No. B08010) are appreciated.

References

[1] M.J.L. Ostergard, C. Clausen, C. Bagger, M. Mogensen, Electrochim. Acta 40 (1995) 1971–1981.
[2] C.W. Tanner, K.Z. Fung, A.V. Virkar, J. Electrochem. Soc. 144 (1997) 21–30.
[3] J.P.P. Huijsmans, F.P.F. van Berkel, G.M. Christie, J. Power Sources 71 (1998) 107–110.
[4] J. Will, A. Mitterdorfer, C. Kleinlogel, D. Perednis, L.J. Gauckler, Solid State Ionics 131 (2000) 79–96.
[5] K. Li, Ceramic Membranes for Separation and Reaction, Wiley, Euro, 2007.
[6] Z.P. Shao, S.M. Haile, Nature 431 (2004) 170–173.
[7] A. Yan, M. Cheng, Y. Dong, W. Yang, V. Maragou, S. Song, P. Tsiakaras, Appl. Catal. B 66 (2006) 64–71.
[8] A. Yan, V. Maragou, A. Arico, M. Cheng, P. Tsiakaras, Appl. Catal. B 76 (2007) 320–327.
[9] H. Hayashi, H. Inaba, M. Matsuyama, N.G. Lan, M.D. okiya, H. Tagawa, Solid State Ionics 122 (1999) 1–15.
[10] T. Nagai, W. Ito, T. Sakon, Solid State Ionics 178 (2007) 3433–3444.
[11] C. Zhu, X. Liu, C. Yi, L. Pei, D. Yan, J. Niu, D. Wang, W. Su, Electrochem. Commun. 11 (2009) 958–961.
[12] G.C. Kostogloudis, C. Ftikos, Solid State Ionics 126 (1999) 143–151.
[13] R. Doshi, V.L. Richards, J.D. Carter, X.P. Wang, M. Krumpelt, J. Electrochem. Soc. 146 (1999) 1273–1278.
[14] A. Mineshige, J. Izutsu, M. Nakamura, K. Nigaki, J. Abe, M. Kobune, S. Fujii, T. Yazawa, Solid State Ionics 176 (2005) 1145–1149.
[15] K.K. Hansen, K.V. Hansen, Solid State Ionics 178 (2007) 1379–1384.
[16] W. Zhou, R. Ran, Z.P. Shao, W.Q. Jin, N.P. Xu, J. Power Sources 182 (2008) 24–31.
[17] A. Mitterdorfer, L.J. Gauckler, Solid State Ionics 111 (1998) 185–218.
[18] L. Yang, C.D. Zuo, S.Z. Wang, Z. Cheng, M.L. Liu, Adv. Mater. 20 (2008) 3280–3283.
[19] L. Yang, Z. Liu, S. Wang, Y. Choi, C. Zuo, M. Liu, J. Power Sources 195 (2010) 471–474.